Pol. J. Environ. Stud. Vol. XX, No. X (XXXX), 1-15
DOI: *10.15244/pjoes/191486* ONLINE PUBLICATION DATE:

Original Research

Entropy Weight Method – Three-Dimensional Motion Modeling of Fog Droplets and Analysis of Influencing Factors

Zhidong Wu[1, 2, 3], Chenming Liu[2], Chuang Li[2], Shuquan Zhang[1]*, Haitao Li[4], Jiaao Zhao[2]

[1]Institute of Economic Crops, Heilongjiang Academy of Agricultural Sciences, Harbin,150086, China
[2]School of Mechanical and Electrical Engineering, Qiqihar University, Qiqihar 161006, China
[3]The Engineering Technology Research Center for Precision Manufacturing Equipment and Industrial Perception of Heilongjiang Province, Qiqihar 161006, China
[4]Qiqihar Branch of Heilongjiang Academy of Agricultural Machinery Sciences, Qiqihar 161000, China

Received: 2 April 2024
Accepted: 22 July 2024

Abstract

A three-dimensional droplet motion model based on droplet motion force and droplet motion evaporation is established to effectively verify the physical and chemical properties of droplets and the impact of external factors on droplet trajectory. Given the influence of multi-influence factors on droplet trajectory and droplet impact, kinematic analysis of a single droplet is conducted through droplet spatial trajectory dimensional transformation to explore the different influences on the droplet in the space of each motion offset direction. Fog droplet trajectory offset is affected by its physical and chemical properties and the external factors. According to the simulation results of the slope of the fitting curve and the coefficient of determination, the entropy weight method is used to analyze the influence of its factors and the fog droplet trajectory offset. The impact of the external wind speed is the largest, but compared with the physical and chemical properties of the droplet, the influence of the droplet trajectory size surpasses the initial angle of incidence. The relevant modeling and simulation conclusions theoretically support the design of fogging systems and optimization of fogging operation parameters.

Keywords: entropy weight method, three-dimensional model of fog droplets, motion trajectory offset

Introduction

The distribution of fog droplets or fog fields directly affects the effectiveness and efficiency of operations. Therefore, analyzing the impact of different factors on fog droplet drift and studying the trajectory and distribution patterns of fog droplets are significant. Currently, abundant research has been conducted on the deposition, drift, and distribution patterns of fog droplets. The combination of spray performance analysis and mathematical modeling can effectively determine

*e-mail: zsq19066568857@163.com
Tel.: +86-13634527227

the relationship between nozzle parameters and atomization parameters, and the introduction of real-time evaluation methods can largely improve the atomization efficiency [1, 2]. A droplet motion model based on the full jet nozzle is established to predict droplet motion trajectory and can effectively verify droplet motion trajectory, water distribution, and droplet radius. The simulation method can effectively verify experiments with different nozzles [3, 4]. During the fogging operation, larger-diameter droplets are less likely to evaporate or drift, but may rebound and roll, resulting in poor fog droplet coverage density, uniformity, and issues such as soil and water pollution, largely reducing the utilization rate of pesticides [5, 6]. In comparison, smaller-diameter droplets have higher adhesion ability, coverage density, and uniformity on the crop surface, but are more prone to drifting and environmental pollution and will cause damage to nearby crops [7]. Reportedly, a rise in relative temperature and humidity accelerates fog droplet evaporation and thereby leads to an increase in fog drift, but to a lesser extent than the fog drift caused by wind speed and direction [8, 9]. Fog droplet size distribution is a critical factor determining the drift of liquid solutions. A smaller fog droplet size leads to a longer stay in the air, a severer effect by the wind field, and faster fog drift [10, 11]. Therefore, studying the influence patterns and factors of fog droplet size, landing points, and motion trajectories is crucial for controlling spray operations, enhancing pesticide efficiency, and optimizing spray parameters.

Investigating the droplet deposition point and trajectory is an important prerequisite for improving atomization efficiency [12-14]. Fog droplet drift during water-based fogging is one of the key factors affecting fogging effectiveness. Fog drift is influenced by the physiochemical properties and size of fog droplets, nozzle structure, wind speed and direction, temperature and humidity, spraying pressure and distance, and other factors [15-18]. Some researchers measured the size parameters and RS of droplets under different combinations of flow rates and wind speeds. Spatial parameters refer to the spraying height and horizontal distance between the target crop and the nozzle. Droplet size distributions are significantly different among different locations [19-21]. For advanced computational fluid dynamics (CFD) two-phase flow spray calculations, specifying the size and velocity distributions of fog droplets is essential in determining boundary conditions [22, 23]. Models predicting the velocity distributions of fog droplets are mainly based on experimental data, where fitting data obtained under different operating conditions is the primary way to analyze fog droplet trajectories [24, 25]. The existing relevant research focuses on establishing analytical models based on single or multiple factors, but does not comprehensively consider spray parameters and spatial parameters. Thus, a multi-factor three-dimensional droplet motion model is required to guide spray operations. Additionally, the accuracy of the polynomial regression model needs to be improved.

Determining the factors affecting droplet landing points and droplet movement trajectories is crucial in analyzing the roles of atomization parameters. The main purpose of this study is to investigate the influence of various factors on droplet motion trajectory and to establish a three-dimensional droplet motion model. The droplet motion trajectories under different influencing factors are simulated and spaced on Matlab. The simulation results are fitted using scatter plots and trend lines, and the key factors influencing the droplet motion trajectory are determined using the entropy weight method. The results serve as the theoretical basis for atomization operations.

Material and Methods

Modeling

Pressure atomization nozzle as a prototype, the impact of environmental parameters, and droplet physical and chemical properties of the settings were simulated using the monitoring parameters and droplet atomization parameters, such as the particle size of a single droplet trajectory offset.

Based on these assumptions combined with the fog droplet trajectory equation, the trajectory of fog droplets within the atomization range was calculated by considering the influence of additional wind speed on fog droplet trajectories. The final landing point of the fog droplets was determined. The displacement offset of fog droplets in each direction during the movement was calculated to analyze the impact of different factors on fog droplet trajectories.

Fog Droplet Motion Model

To effectively verify the forces acting on fog droplets during motion, a force analysis was conducted

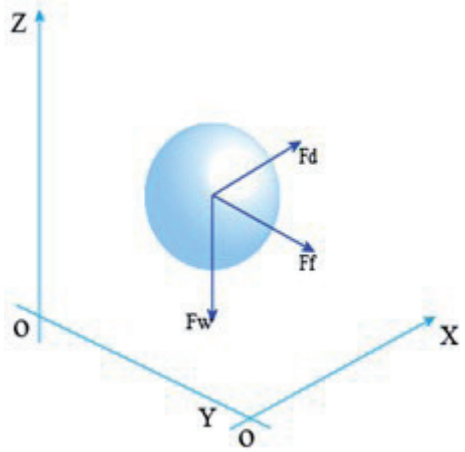

Fig. 1. Diagram of fog droplet forces.

on individual fog droplets to facilitate the analysis of the main forces at work. Fog droplets are always subjected to the combined forces of gravity, air drag, and buoyancy during motion. The force diagram of a fog droplet is shown in Fig. 1 for the analysis of forces during movement.

A mixed solution is pressurized into the nozzle through a water pump in the atomization system. When sprayed out of the nozzle, the solution forms droplets in diameter at the micrometer range. Then the energy and volume changes of individual droplets were investigated. According to the law of conservation of energy, a balance during the falling of the droplets is reached among the gravitational force F_w acting on the droplet, buoyant force F_f, and air drag force F_d. This balance is calculated using Equation (1):

$$\mathrm{m}\frac{dv}{dt} = F_f + F_d + F_w \tag{1}$$

The equations for m, F_f, and F_d in Equation (1) are as follows:

$$m = \frac{4}{3}\pi\left(\frac{D}{2}\right)^3 \cdot \rho_h \tag{2}$$

$$F_f = \frac{4}{3}\pi\left(\frac{D}{2}\right)^3 g \cdot \rho_a \tag{3}$$

$$F_d = \frac{1}{2}C_d\rho_h\left(\frac{D}{2}\right)^2 \pi v^2 K \tag{4}$$

where D is the diameter of a single fog droplet in the mixed solution, v is the final velocity of the falling droplet, K is the air viscosity coefficient, $\boldsymbol{\rho}_a$ is the air density, and $\boldsymbol{\rho}_h$ is the density of the mixed solution.

Substituting Equation (3) into Equation (4) yields:

$$\frac{4}{3}\pi\cdot\left(\frac{D}{2}\right)^3 \cdot \rho_h \cdot g = \frac{4}{3}\pi\cdot\left(\frac{D}{2}\right)^3 \cdot \rho_a \cdot g + 6\pi\cdot\left(\frac{D}{2}\right)\cdot K \cdot v \tag{5}$$

Further simplification reveals the relationship between droplet diameter and droplet falling velocity as follows:

$$D = 2\sqrt{9\cdot K\cdot v\cdot\Delta\rho\cdot g} \tag{6}$$

Approximating the fog droplet as a spherical body, its mass m can be calculated using Equation (7):

$$m = \frac{\rho_h}{6}\cdot\pi\cdot D^3 \tag{7}$$

The Reynolds number R_e can be calculated from Equation (8):

$$R_e = \frac{\rho_h \cdot v_R \cdot d}{\mu} \tag{8}$$

where d is characteristic dimension (characteristic length), v_R is the relative velocity of gas to liquid, and $\boldsymbol{\mu}$ is the dynamic viscosity of air. $\boldsymbol{\mu}$ can be calculated as follows:

$$\mu = \nu\cdot\rho \tag{9}$$

where v is kinematic viscosity and is computed as follows:

$$\nu = \eta\cdot\rho \tag{10}$$

where $\boldsymbol{\eta}$ is dynamic viscosity.

Air resistance is one of the key factors affecting droplet movement. The air resistance coefficient C_d is closely and linearly related to R_e,, and is calculated as follows:

$$C_d = \frac{f}{\frac{1}{2}\rho\cdot U^2\cdot\pi\cdot a^2} \tag{11}$$

The result of using the Oseen correction for C_d is:

$$C_d = \frac{24}{R_e} + \frac{9}{2} \tag{12}$$

Kinematic modeling for droplet motion in directed airflow:

The droplets during motion are subjected to various forces, which complicates the analysis of droplet motion laws. To highlight the characteristics of the main forces and facilitate kinematic modeling for droplet motion, a kinematic model for droplet motion in directed airflow of the misting system is established by considering the greenhouse as a closed environment. During the atomization without external influence, a model for droplet motion in directed airflow is established by relying on the greenhouse environment and the properties of the droplets:

$$m_p\cdot\frac{dv_p}{dt} = \frac{C_d\cdot R_e}{24}\cdot F_d + F_w \tag{13}$$

$$F_w = m_p\cdot g = \frac{1}{6}\cdot\pi\cdot d_p^3\cdot\rho_p\cdot g \tag{14}$$

$$F_D = \frac{6\cdot\pi\cdot\mu_f\cdot d_p}{C_e}\left(v_f - v_p\right) \tag{15}$$

where F_w is the gravity of a single droplet, N; F_d is air drag force, and N; C_e is the Cunningham slip correction factor (typically 1.489).

To verify the characteristics of the main forces acting on droplet motion, a three-dimensional droplet motion model is established based on the ballistic theory with the following equations of motion:

$$\int m \cdot \frac{du_x}{dt} = -\frac{1}{2} C_d \cdot \rho_a \cdot V_R^2 \cdot A \cdot e_x + m \cdot \frac{dv}{dt} \quad (16)$$

$$\int m \cdot \frac{du_y}{dt} = -\frac{1}{2} C_d \cdot \rho_a \cdot V_R^2 \cdot A \cdot e_y + m \cdot \frac{dv}{dt} \quad (17)$$

$$\int m \cdot \frac{du_z}{dt} = -\frac{1}{2} C_d \cdot \rho_a \cdot V_R^2 \cdot A \cdot e_z + m \cdot g - \frac{\rho_a}{\rho_h} \cdot m \cdot g + m \cdot \frac{dv}{dt} \quad (18)$$

where m is the mass of a single droplet in the mixed solution; u_x, u_y, and u_z are the x-, y-, and z-direction velocity components of the droplet, respectively, *m/s*; t is the flight time of the droplet in the air; V_R is the relative motion speed of the droplet to air; A is the surface area of the droplet; e_x, e_y, and e_z represent the x-, y-, and z-direction unit vectors of velocity, respectively; g is the acceleration due to gravity. The V_R of a single droplet in a mixed solution is determined as follows:

$$V_R = \sqrt{u_x^2 + u_y^2 + u_z^2} \quad (19)$$

In the water-herb mixed solution, the e_x, e_y, and e_z of a single droplet are:

$$\begin{aligned} e_x &= \frac{u_x}{V_R} \\ e_y &= \frac{u_y - w}{V_R} \\ e_z &= \frac{u_z}{V_R} \end{aligned} \quad (20)$$

The impact of various factors (including external wind speed) on the motion behavior of droplets in atomization is analyzed in order to solve the situation of individual droplet forces in the x, y, and z directions within a three-dimensional coordinate system.

Droplet motion and evaporation model:

The droplets during motion are subjected to their physical and chemical properties, environmental factors, and external influences that lead to motion evaporation. This subjection results in changes in droplet size during motion, affecting the trajectory. The droplet evaporation rate during motion evaporation is computed as follows:

$$\frac{dm}{dt} = 4 \cdot \pi \cdot r^2 \cdot D_v \cdot \frac{d\rho}{dr} + Y_v \cdot \frac{dm}{dt} \quad (21)$$

The mass transfer rate of the fluid is expressed as:

$$\frac{dm}{dt} = \frac{n}{n-1} \cdot 2 \cdot \pi \cdot r \cdot \rho_h \cdot sh \cdot \ln\left(\frac{1 - Y_\infty}{1 - Y_S}\right) \quad (22)$$

The changing rate of droplet radius is:

$$\begin{aligned} \frac{dr}{dt} &= \frac{n}{n-1} \cdot \frac{sh \cdot \rho_h \cdot D_v}{2 \cdot \rho_d \cdot r} \ln\left(\frac{1 - Y_\infty}{1 - Y_s}\right) \\ &= \frac{n}{n-1} \cdot \frac{sh \cdot \rho_h \cdot D_v}{2 \cdot \rho_d \cdot r} \cdot \ln(1 + Bm) \end{aligned} \quad (23)$$

where Bm is Sherwood mass transfer number, sh is Sherwood number, sh is Sherwood number, and D_v is diffusion coefficient (determined based on environmental parameters at the time of model solving).

Entropy Weight Method

Based on the objective entropy weight method, the main forces acting on the droplets during movement are verified, and the trajectory of droplet movement and the weight proportion of each factor are analyzed. For n samples and m indicators, let x_{ij} be the j-th indicator of the i-th sample (i = 1, 2, 3, …, n; j = 1, 2, 3 ,…, m). The calculation steps are as follows:

$$x_{ij} = \frac{\max\{x_{1j}, x_{2j}, \ldots, x_{nj}\} - x_{ij}}{\max\{x_{1j}, x_{2j}, \ldots, x_{nj}\} - \min\{x_{1j}, x_{2j}, \ldots, x_{nj}\}} \quad (24)$$

$$p_{ij} = \frac{x_{ij}}{\sum_{i=1}^{n} x_{ij}}, (i = 1,2,\ldots, \quad n; j = 1,2,\ldots, \quad m) \quad (25)$$

$$e_j = -k \cdot \sum_{i=1}^{n} p_{ij} \cdot \ln(p_{ij}), \quad k = \frac{1}{\ln(n)} > 0, j = 1,2,\ldots,m \quad (26)$$

$$d_j = 1 - e_j, j = 1,2,\ldots\ldots,m \quad (27)$$

$$w_j = \frac{d_j}{\sum_{i=1}^{n} d_j}, j = 1,2,\ldots,m \quad (28)$$

where p_{ij} is the weight of the *i-th* sample under the *j-th* indicator, e_j is the entropy of the *j-th* indicator, k is an intermediate variable, d_j is the information entropy redundancy of the *j-th* indicator, and w_j is the weight of each indicator.

The constant-speed aerodynamics model is improved, and the influence of external wind speed on

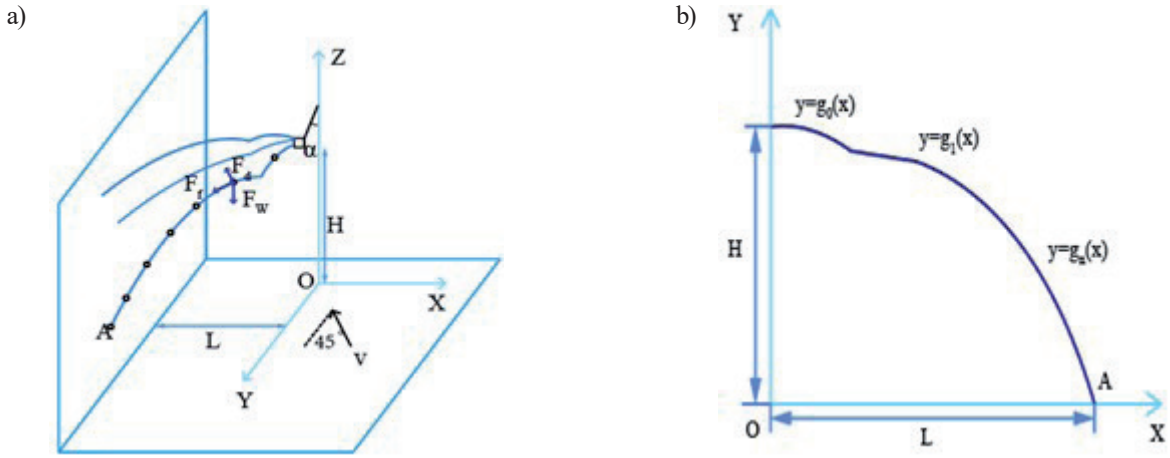

Fig. 2. Trajectories of droplet motion. *H*, installation height of the nozzle, cm; ***α***, angle between the nozzle and the extension rod; *A*, final landing point of the droplet, cm; *L*: horizontal flight distance, cm; *a*: initial directional acceleration, m/s^2; *g*, acceleration due to gravity, m/s^2; *v*, external wind speed, m/s; $g_0(x)$, initial trajectory curve of droplet motion; $g_n(x)$, trajectory curve of droplet motion with the support of external wind speed; *O*, the plane where the crop leaves are located. a) Motion trajectory and forces acting on droplets in three-dimensional space. b) Motion trajectory of droplets in a two-dimensional Cartesian coordinate system.

the movement of droplets is considered. According to the three-dimensional motion equation of droplets, the spatial coordinates of the same fog droplet at different moments are calculated, and the movement trajectory of droplets in space based on the coordinates is fitted. A polynomial can be used to fit the droplet movement trajectory curve that is similar to a parabola during droplet movement. The coefficients of the polynomial can be calculated using the least squares method as follows:

$$f_n(x) = a \cdot x^m + b \cdot x^{m-1} + \cdots + n \cdot x^{m-t} \tag{29}$$

Based on the relationship between the final landing point of the droplet trajectory on the atomization surface and the flying distance of the droplet, the motion trajectory in the three-dimensional Cartesian coordinate system of the droplet is transformed into the motion trajectory in its two-dimensional Cartesian coordinate system. The schematic diagram of the droplet trajectory is shown in Fig. 2.

Model Solving

The droplet motion model is programmatically processed on Matlab as the development tool. The flow chart of the droplet motion model is shown in Fig. 3.

The accuracy of the three-dimensional motion model of fog droplets was verified on Matlab. Before the model verification, environmental parameters were introduced, and the parameters of the fog droplets were set up. Deterministic variables such as the initial incidence velocity of the droplet were introduced, and the factors influencing the trajectory offset were sequentially introduced. According to the simulation results, a fog droplet motion trajectory curve was plotted. Then the entropy weight method was used to analyze the simulation results and determine the weight of each factor.

Simulation Results and Analysis

Simulated Parameters for Simulation.

Based on the droplet distribution calculation model as established, pressure-type atomization nozzles were taken as the research object to analyze the effects of different angles and external wind speeds on the atomization efficiency. The American Society of Agricultural Engineering (ASAE) droplet size classification criteria were introduced (Table 1) to determine the effect of droplet size on droplet trajectory. The simulated factor levels are shown in Table 2, and the simulated operating parameters of the nozzle and environmental parameters are shown in Table 3.

Model Verification

Motion Trajectory

The environmental parameters required for simulation were defined, and the droplet trajectories under different influencing factors were simulated on Matlab to effectively verify the correctness of the droplet motion model. Fig. 4 shows the simulation results of droplet motion trajectories under the nozzle working pressure of 1 MPa, external wind speed of 0.5 m/s, initial incident angle of 15°, and different concentrations and particle sizes of droplets. The simulation curves of droplet motion trajectories show when the droplet is in the wind zone, the motion trajectory is related to its concentration, particle size, and initial position. The motion trajectory of the droplet in the wind zone

is most affected by the wind speed. The trajectory curve of droplets under different wind speed conditions is shown in Fig. 5.

The motion trajectories of the droplets are all in the form of parabolas. As the droplet diameter increases, the motion trajectories become smoother and the flight distance is longer. Based on the simulation results considering influencing factors and the environment, the simulated motion trajectories are similar to those in actual atomization operations. As for the curve changes of droplet offset in different directions, the offset of droplet motion trajectories varies under different influencing factors. Under the additional influence of wind speed, factors such as particle size, droplet concentration, and the initial angle of droplet movement all affect the offset of droplet motion trajectories.

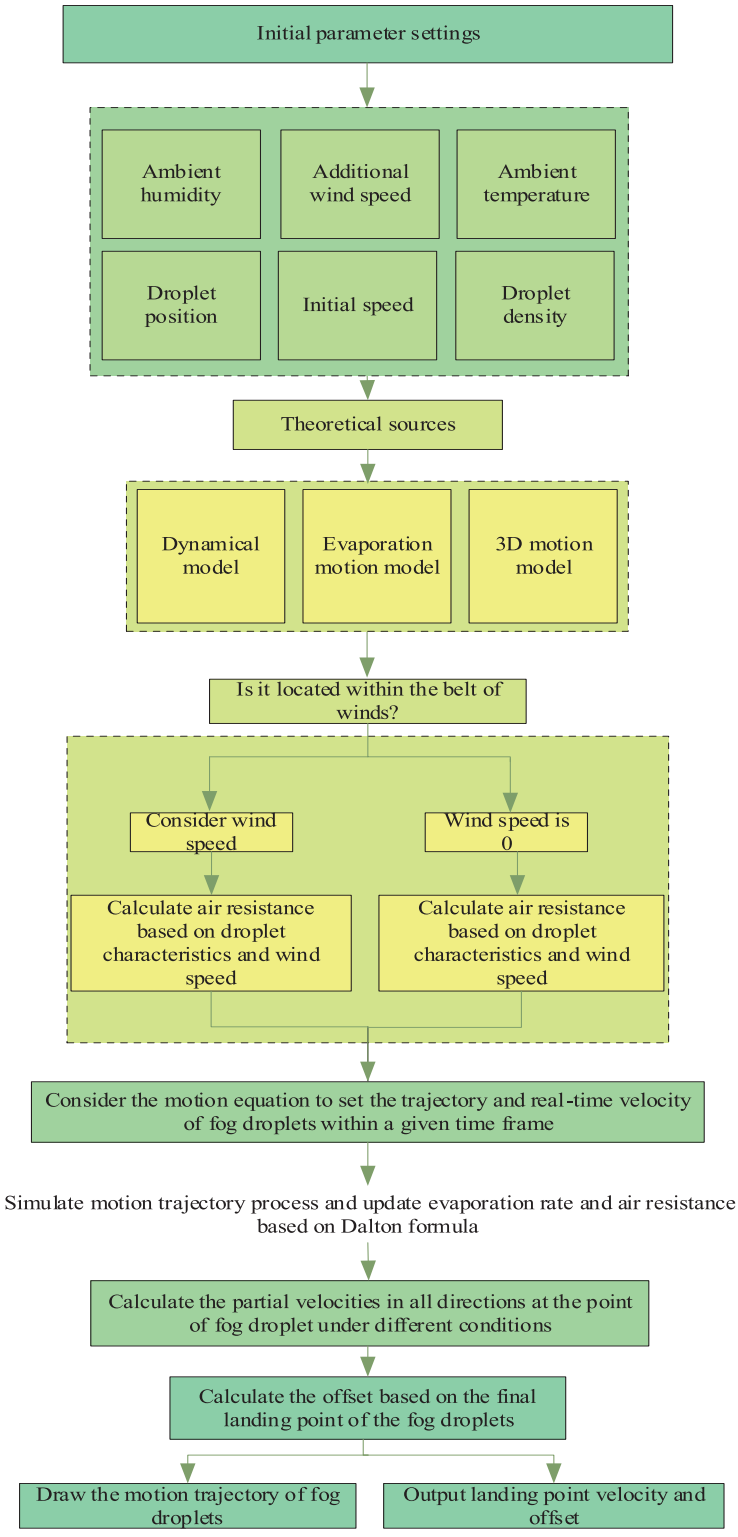

Fig. 3. Flowchart of droplet motion model solving.

Table 1. ASAE Classification standard for fog droplet diameter.

Criteria for classification	Symbol abbreviation	Volume center diameter (μm)
Very fine droplets	VF	<100
Droplet	F	100-175
Medium droplets	M	175-250
Thick mist droplet	C	250-375

On the simulated curves of droplet motion trajectories, droplets of different sizes have different final landing points. However, the droplets in diameter of 140 μm vary the most severely in terms of landing points compared to the droplets of other sizes. Let the initial coordinates of the droplets be (0, 0, 1). Then the changing trend in droplet motion trajectory offsets was analyzed. The entropy weight method was used to analyze the main influencing factors of droplet motion trajectory offsets.

The influencing factors affecting droplet motion trajectories include both intrinsic physiochemical properties and external factors. In addition to intrinsic physiochemical properties, the initial movement angle of the droplets also influences droplet motion trajectories. The motion trajectory curves for droplets with different initial movement angles are shown in Fig. 6.

Analysis of Influencing Factors in Droplet Motion Trajectory Simulation

With the entropy weight method, the factors influencing droplet motion trajectories were analyzed. The method of variable controlling was employed to analyze the impact of each factor on droplet motion trajectories, which theoretically underlie the development of atomization systems and precise atomization.

Droplet Concentration

Table 4 presents the influence of droplet concentration on motion trajectories using the entropy weight method, with other parameters set at a working pressure of 1 MPa.

The motion trajectories of droplets of the same particle size were chosen at the same initial position and wind speed condition but with different concentrations. Totally 17 sets of *X*- and *Y*-axis droplet motion trajectory offsets at the same nodes were selected for analysis. The offset curves are shown in Fig. 7.

The influence of fog droplet concentration on droplet motion trajectories was analyzed. Curve fitting was performed on simulated displacement to determine the slope and determination coefficient of the fitting curve (Table 5).

According to the curves of trajectory displacement on each axis along with the corresponding slope and determination coefficient, the fitted curves of fog droplet trajectory displacement have relatively close slopes. This result indicates changes in fog droplet concentration impact the trajectory displacement to a certain extent, but very slightly. Given that the change in fog droplet volume due to changes in fog droplet size exponentially grows, the displacement of larger droplets is larger. Nevertheless, the overall trends of motion displacement remain largely consistent.

Table 2. Factors and levels in simulation.

Level	Droplet diameter / μm	Working pressure / MPA	Additional wind speed / m/s	Concentration of fog droplets	Incident angle
1	40, 80, 140, 180, 240, 280	1.0	0.5, 1, 1.5, 2, 2.5, 3	$1.0_{*}10^{3}$	5°, 10°, 15°
2	40, 80, 140, 180, 240, 280	1.0	0.5, 1, 1.5, 2, 2.5, 3	$1.04_{*}10^{3}$	5°, 10°, 15°
3	40, 80, 140, 180, 240, 280	1.0	0.5, 1, 1.5, 2, 2.5, 3	$1.08_{*}10^{3}$	5°, 10°, 15°
4	40, 80, 140, 180, 240, 280	1.0	0.5, 1, 1.5, 2, 2.5, 3	$1.12_{*}10^{3}$	5°, 10°, 15°
5	40, 80, 140, 180, 240, 280	1.0	0.5, 1, 1.5, 2, 2.5, 3	$1.16_{*}10^{3}$	5°, 10°, 15°
6	40, 80, 140, 180, 240, 280	1.0	0.5, 1, 1.5, 2, 2.5, 3	$1.20_{*}10^{3}$	5°, 10°, 15°

Table 3. Nozzle operating parameters and environmental parameters for simulating droplet motion trajectories.

Parameters	Value	Parameters	Value
Nozzle diameter mm	0.5	Diffusion of water vapor molecules mol*L^{-1}	18
Height above ground cm	100	The average molecular weight of mixed air mol*L^{-1}	29
Air temperature ℃	25	Relative humidity %	60
Atmospheric pressure kph	101.325	Concentration of fog droplets kg*m^{-3}	$1.0\text{-}1.2_{*}10^{3}$

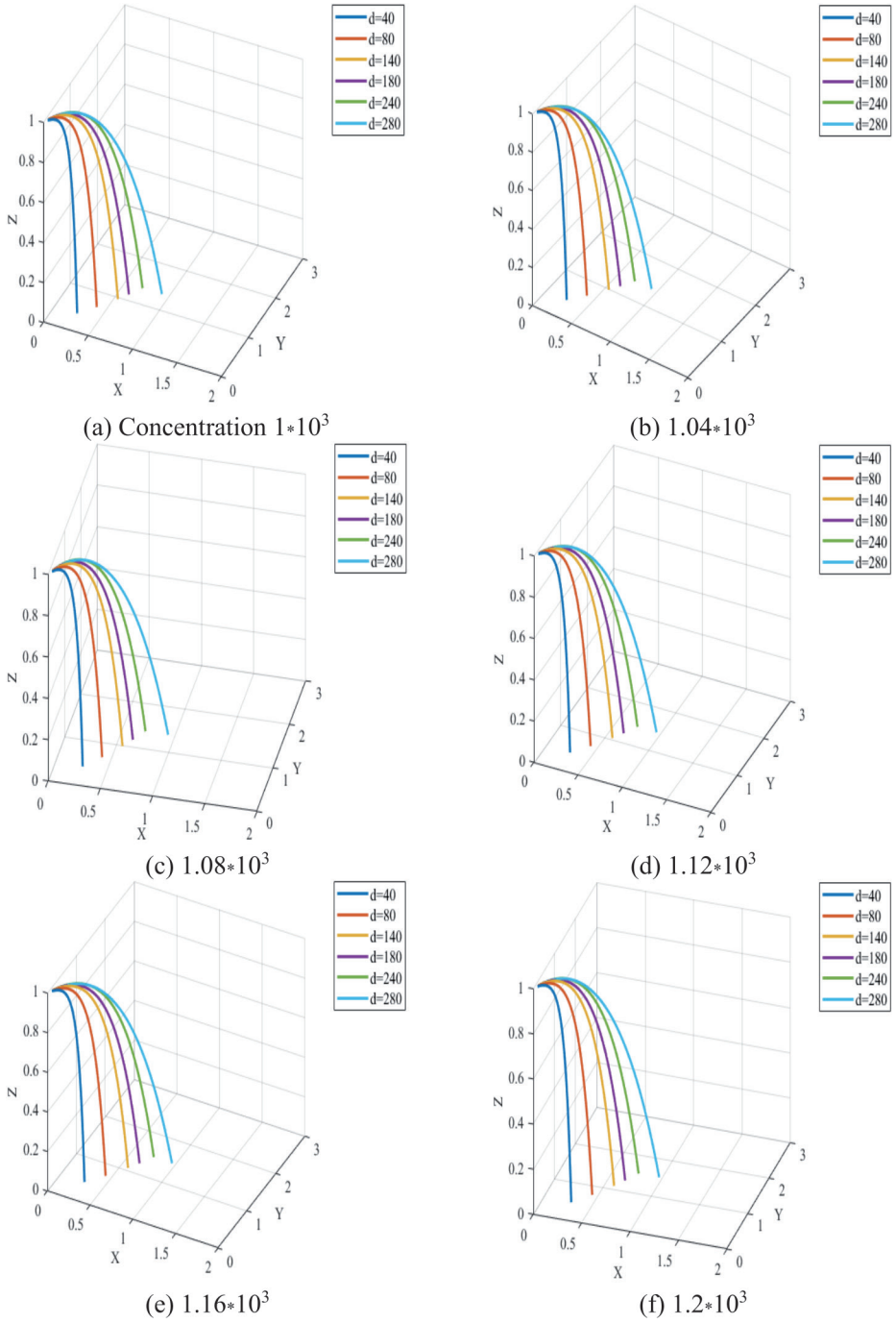

Fig. 4. Curves of motion trajectories of droplets with different concentrations and particle sizes.

Different Particle Sizes

Table 6 illustrates the impact of droplet concentration on droplet trajectory analyzed using the entropy weight method, with the working pressure set at 1 MPa and other parameters configured accordingly.

Droplet trajectories with different sizes but the same initial position and concentration under the same wind speed were selected to effectively analyze the influence of physical and chemical properties on droplet trajectory. Seventeen sets of *X*-axis and *Y*-axis droplet trajectory offsets for the same nodes were analyzed. The offset curves are shown in Fig. 8.

The effect of fog droplet size on fog droplet motion trajectory was analyzed, and curve fitting of fog droplet trajectory displacement changes was conducted. The slope and determination coefficient of the fitted curve are shown in Table 7.

Results in Table 7 show that the fog droplet motion trajectory displacement is related to the droplet size. The trajectory displacement of larger droplets is larger, and the speed of displacement at initial time increases with the droplet size. Additionally, the change in slope of the fitted curve varies more rapidly with droplet size

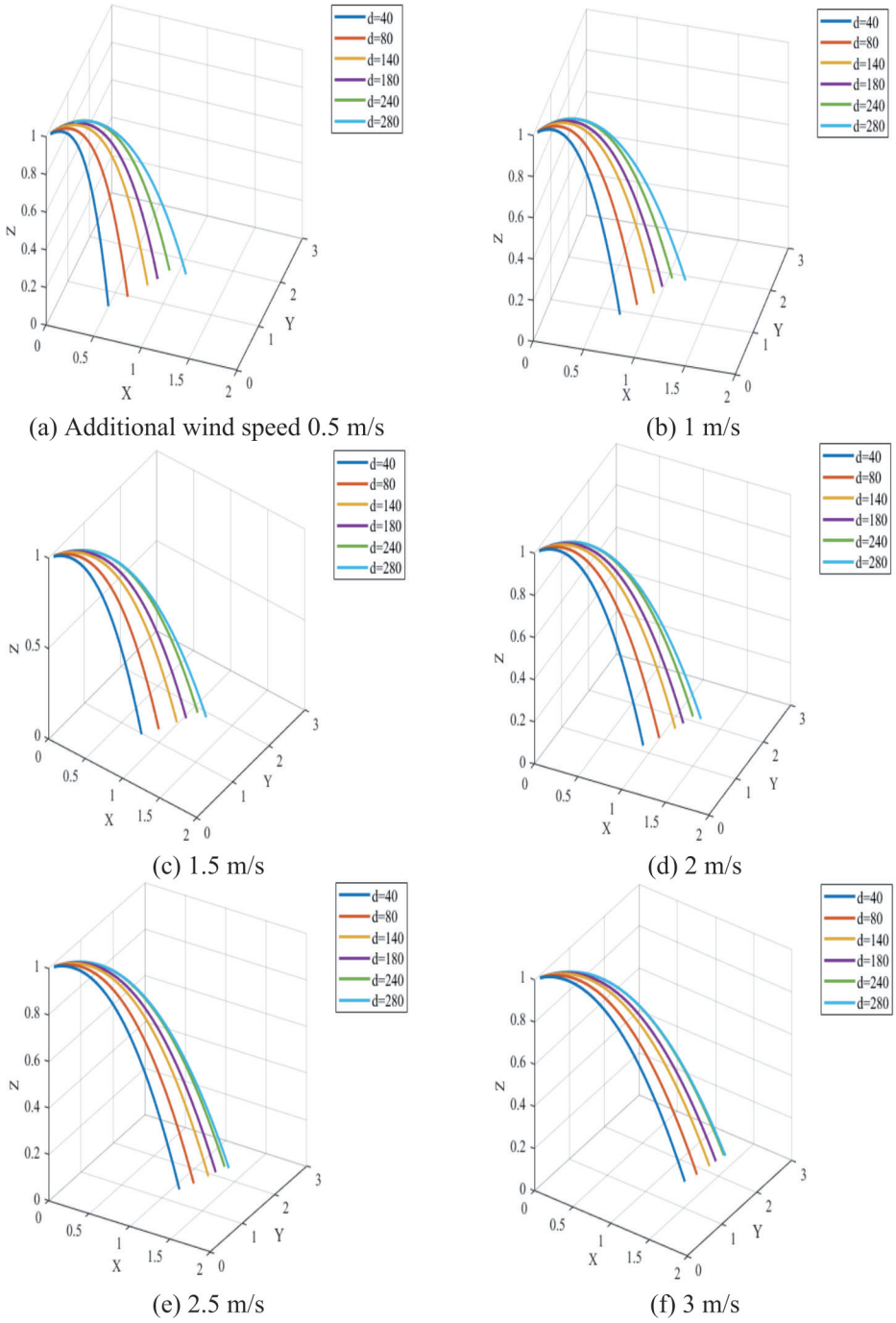

Fig. 5. Curves of motion trajectories of droplets under different wind speeds.

compared to the effect of concentration on fog droplet motion trajectory. Entropy weighting analysis under consistent boundary conditions reveals that fog droplet motion trajectory is significantly influenced by droplet size.

Initial Angle

Table 8 demonstrates the influence of the initial angle of droplet motion on droplet trajectory under a working pressure of 1 MPa with the other set parameters using the entropy weight method.

The impact of external factors on droplet trajectory involves changing the initial angle of droplet motion (equivalent to altering the initial position in projectile motion) to observe the object motion trajectory. Under the same wind speed and droplet size and different initial motion angles, the droplet motion trajectories at the same concentration were selected for analysis at the same nodes with a time interval of 0.015 seconds along the *X*- and *Y*-axis. Totally 17 groups of droplet trajectory offset data were analyzed, and the offset curves are shown in Fig. 9.

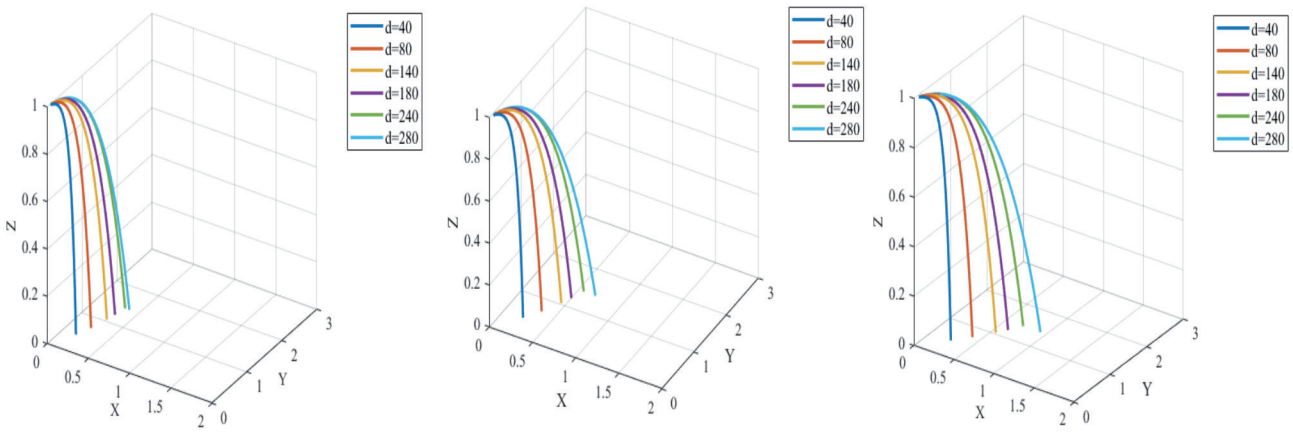

(a) Droplet initial movement angle of 5° (b) 10° (c) 15°

Fig. 6. Curves of motion trajectories of droplets with different particle sizes under various initial movement angles.

Table 4. Setting parameters for analyzing the influence of concentration.

Analytical Parameters	Fixed Parameters				
Concentration of fog droplets	Initial position coordinates	Particle size	Additional wind speed	Initial incidence angle	Wind bandwidth
1.0-1.2$_*$10^3	(0, 0, 1)	80 μm	0 m/s	15 °	30 cm

Table 5. Fitted curve slope and determination coefficient.

X-axis trajectory displacement		*Y*-axis trajectory displacement	
The slope of the fitted curve	R^2	The slope of the fitted curve	R^2
0.0183	0.9609	0.0298	0.898
0.0187	0.9624	0.0306	0.9003
0.0191	0.9637	0.0315	0.9025
0.0195	0.9650	0.0324	0.9047
0.0198	0.9662	0.0332	0.9067
0.0201	0.9663	0.0342	0.911

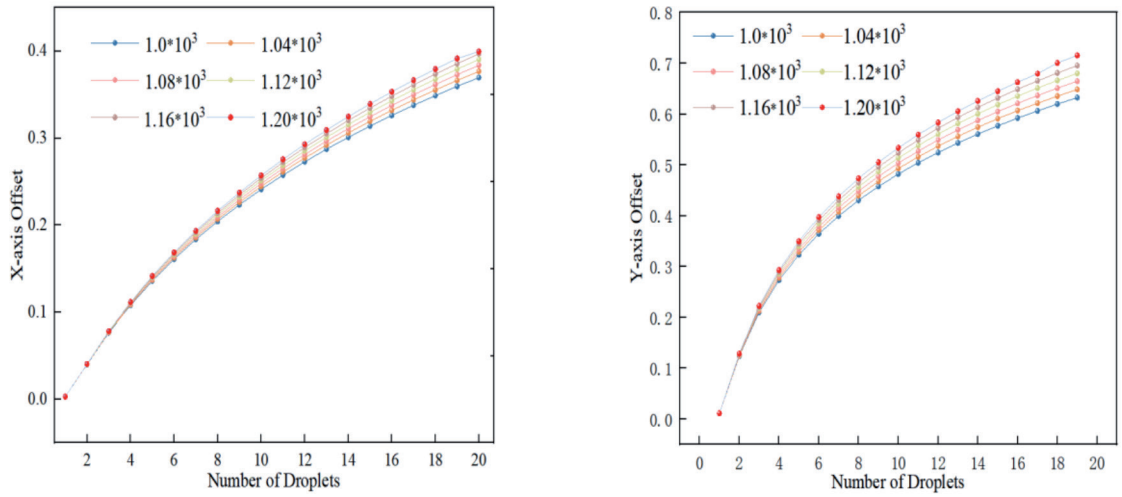

(a) *X*-axis offset (b) *Y*-axis offset

Fig. 7. Line charts of trajectory offset of droplets at different concentrations.

Table 6. Analysis of parameters set for studying the impact of droplet size on droplet trajectory.

Analytical parameters	Fixed parameters				
Particle size μm	Initial position coordinates	Concentration of fog droplets	Additional wind speed	Initial incidence angle	Wind band width
40, 80, 140, 180, 240, 280	(0, 0, 1)	$1.12*10^3$	0 m/s	15 °	30 cm

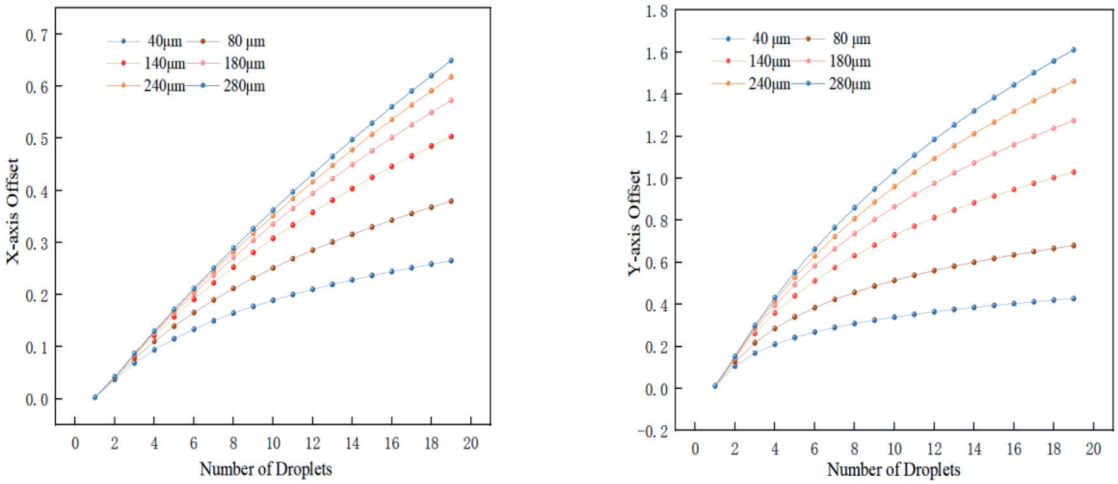

(a) *X*-axis offset (b) *Y*-axis offset

Fig. 8. Scatter plots of droplet trajectory offset for different droplet sizes.

Table 7. Fitted curve slope and determination coefficient.

X-axis trajectory displacement		*Y*-axis trajectory displacement	
The slope of the fitted curve	R^2	The slope of the fitted curve	R^2
0.0134	0.09382	0.0189	0.8519
0.02	0.9668	0.3024	0.9047
0.0274	0.9851	0.0521	0.9415
0.0315	0.9914	0.0665	0.9589
0.0341	0.9944	0.0775	0.9691
0.0364	0.9964	0.0863	0.9758

Table 8. Analysis of parameters set for analyzing the influence of droplet motion initial angle.

Analytical parameters	Fixed parameters				
Initial incidence angle	Initial position coordinates	Particle size	Additional wind speed	Concentration of fog droplets	Wind band width
5°, 10°, 15°	(0, 0, 1)	80 μm	0 m/s	1.12_*10^3	30 cm

The effect of the initial incidence angle of fog droplets on the motion trajectory was analyzed through curve fitting of the simulated data. The results for the fitted curve slope and determination coefficient are provided in Table 9.

Results in Table 9 show that the displacement of fog droplet trajectories along different axes varies under varying angles. The initial angle affects the *X*-axis displacement notably, but less significantly influences the *Y*-axis displacement. This effect is related to the initial incidence angle within the *XY* plane. However, comprehensive analysis indicates that the angle impacts fog droplet displacement to a certain extent, and this impact surpasses that of the inherent physical and chemical properties on displacement.

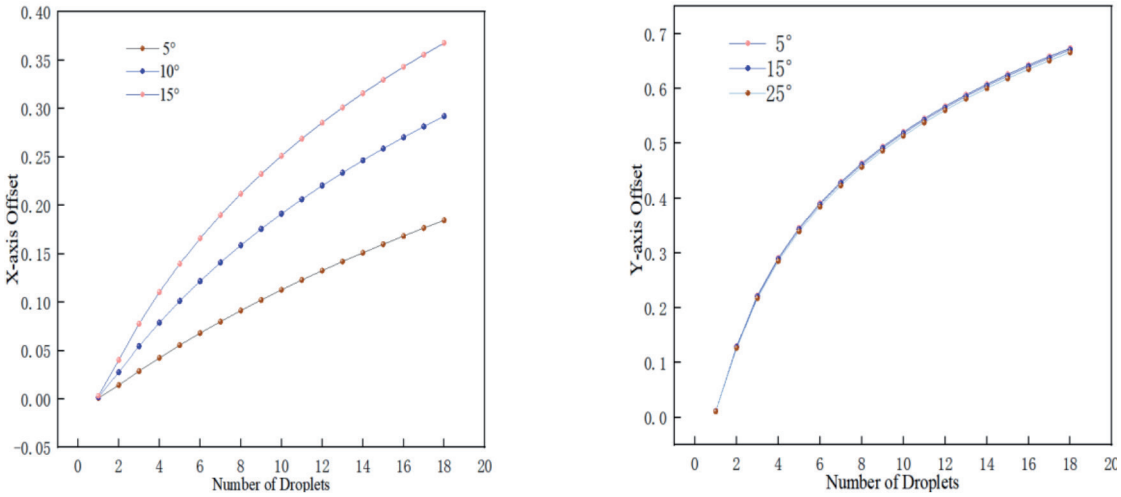

(a) *X*-axis offset (b) *Y*-axis offset

Fig. 9. Scatter plot of droplet trajectory offset at different initial motion angles.

Table 9. Fitted curve slope and determination coefficient.

X-axis trajectory displacement		*Y*-axis trajectory displacement	
The slope of the fitted curve	R^2	The slope of the fitted curve	R^2
0.0107	0.992	0.0341	0.9059
0.0167	0.98	0.034	0.9066
0.0206	0.9687	0.0338	0.9077

External Wind Speed

Table 10 uncovers the impact of external wind speed on droplet trajectory analyzed using the entropy weight method under a working pressure of 1 MPa and the set of other parameters.

The impact of external factors on droplet movement trajectory was analyzed by changing the external wind speed to observe the object movement trajectory. The droplet movement trajectorys with the same particle size, initial movement angle, and concentration were selected for analysis under different wind speeds. Seventeen sets of *X*- axis and *Y*-axis droplet trajectory offset data at the same nodes with a time interval of 0.015 seconds were selected. The data selected are all for droplets in motion in simulated wind belt positions. The trajectory offset curves are shown in Fig. 10.

When the influence of wind speed on fog droplet motion trajectories was analyzed, conditions were set consistently while varying wind speed magnitude. The displacement of fog droplet motion trajectories was observed under different wind speeds, and the slope and determination coefficient of the displacement at different nodes were determined through curve fitting (Table 11).

On the curves and fitted curve slopes, when fog droplets are positioned within the wind zone, the different wind speeds evidently affect the droplet motion trajectories. As the wind speed changes, the slope of the fitted curve for the displacement output at different nodes changes noticeably. Wind speed significantly impacts the displacement of fog droplet motion, which is far severer compared with the inherent physical and chemical properties or the initial incidence angle.

Discussion

To improve the effects of fogging operation and plant protection operation and to design perfect plant protection operation equipment, it is necessary to simulate the corresponding environmental parameters in the plant protection operation and improve the technical parameters required for plant protection operation according to theories. Aiming at the issues in atomization operations (e.g., small quality of fog droplets, difficulty in controlling), relevant experts have identified the main factors affecting fog droplet trajectories, including droplet size and external influencing factors. However, model simulation has not been used in fog droplet trajectory analysis. Chen et al. demonstrated the effects of droplet sizes on droplet motion deposition and drift, analyzed the distribution of internal wind force in spraying, and determined the optimal droplet size and related spraying parameters [10]. Factors affecting the effectiveness of atomization operations include physical and chemical properties,

Table 10. Analysis of parameters set for analyzing the impact of external wind speed.

Analytical parameters	Fixed Parameters				
Additional wind speed m/s	Initial position coordinates	Particle size	Initial incidence angle	Concentration	Wind band width
0.5, 1, 1.5, 2, 2.5, 3	(0, 0, 1)	80 μm	15°	$1.12_{*}10^{3}$	30 cm

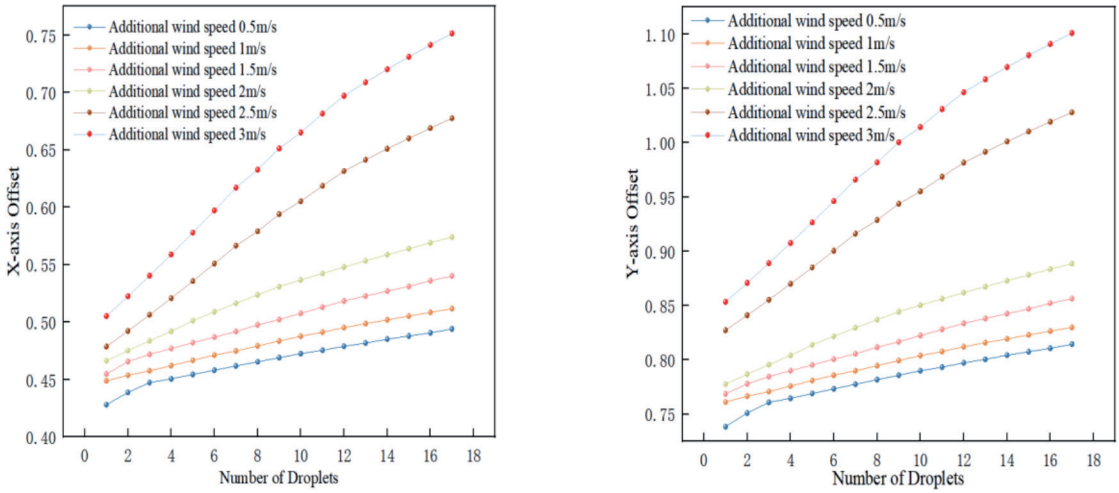

(a) *X*-axis offset (b) *Y*-axis offset

Fig. 10. Scatter plots of droplet trajectory offset at different wind speeds.

Table 11. Fitted curve slope and determination coefficient.

X-axis trajectory displacement		*Y*-axis trajectory displacement	
The slope of the fitted curve	R^2	The slope of the fitted curve	R^2
0.0292	0.985	0.04	0.9732
0.0377	0.9943	0.0485	0.9764
0.0457	0.9975	0.0582	0.9758
0.0531	0.9982	0.0679	0.9829
0.0592	0.9974	0.0776	0.9875
0.0629	0.9976	0.0873	0.9906

droplet particle size, and external wind speed, all of which influence droplet drift [15].

The external factors and the intrinsic properties of droplets during atomization that affect droplet trajectory were considered so as to improve the fixed-speed airflow dynamics model. The three-dimensional motion trajectories were transformed into lower dimensions, and droplet trajectory offsets were calculated, which were the basis of subsequent analyses. According to the principle of droplet equilibrium before and after atomization, the droplet trajectory model in the space was established, and the entropy weighting method was used to analyze the impact of the factors on droplet trajectory in the atomization. Model validation indicates the directional movement offsets during droplet movement differently affect the trajectories of droplets in different sizes with factors such as nozzle angle and external wind speed, which is consistent with the conclusions from Mcginty, J. A. et al. [16]. However, the model also has some shortcomings. First, it is established under ideal conditions considering environmental factors, while the actual operations of the nozzle hydraulic characteristics are different from the set parameters in the simulation, which may impact the simulation accuracy to a certain extent. According to the environmental parameters and the physiochemical properties of droplets, the droplet kinematics model was established, and the influence of each factor on droplet trajectory was analyzed using the entropy weight method. According to the droplet movement trajectory offsets in all directions, the design

and use of the atomization system can be optimized based on the simulation results of the model.

To effectively verify the influence of different factors on fog droplet trajectories, Balsari, P. et al. established a droplet motion model based on single-factor influence without considering spraying parameters and spatial parameters [19]. Therefore, it is necessary to optimize the droplet motion model and consider multiple factors comprehensively. Other researchers employed CFD to validate the droplet distributions and emphasized that droplet size and velocity distributions were important parameters for accurate validation [20, 23].

The findings of this study reveal some conditions for the agricultural applications of the atomization equipment, the technical parameters to be considered during use, relevant factors affecting the effectiveness of use, and the method of model establishment. It has reduced to some extent the resource waste brought by theoretical production equipment, enabling better transformation of theoretical deductions. The required parameters and related hardware parameters can be simulated by relying on relevant simulation software, and the simulation results have a certain reference value, thereby confirming the accuracy of theoretical deductions. Model establishment combined with the entropy weight method can be used to comprehensively analyze the influencing factors of droplet trajectories and highlight the main influencing factors, providing technical support and theoretical guarantee for the production of related equipment. The focus of future work will be to explore the impact of different influence factors on fog droplet distribution, comprehensive consideration of fog droplet distribution modeling, the establishment of an iterative parameter-based fog droplet distribution model, improvement of fogging operation, and the plant canopy deposition rate.

Conclusions

The trajectories of droplets in different particle sizes were calculated based on the three-dimensional trajectory equation of the droplets and by considering the droplet force, evaporation of droplet motion, and the influence of various factors. The entropy weighting method was used to analyze the ratio of the influencing factors on the droplet trajectory and calculate the droplet trajectory offset in the three-dimensional space in various directions, so as to determine the influencing factors on the droplet trajectory. The simulation results were fitted with scatter plots and trend lines. The slopes of the fitted curves and the coefficients of determination show that the curve slope of droplet trajectory offset at different moments varies most obviously under the influence of wind speed, and the coefficient of determination is the largest, indicating droplet trajectory is most obviously affected by wind speed. Comparison of the curve slopes and the rest of the influencing factors shows that droplet diameter is more influential than the initial particle size, and angle of incidence is more influential than droplet concentration. The error analysis of the trajectory offset and comparison of trajectory offset at the same moment indicate the three-dimensional motion model of fog droplets can effectively analyze the factors affecting the droplet trajectory. The three-dimensional droplet motion model has certain reliability and is suitable for designing atomization systems and optimizing spray parameters.

Author Contributions

All authors contributed to the manuscript. Conceptualization, C.L. and Z.W.; methodology, Z.W.and C.L.; validation, C.L. and C.L., Z.W. All authors have read and agreed to the published version of the manuscript.

Acknowledgments

This work was supported by the Basic Research Fund for State-owned Universities in Heilongjiang Province (No. l45209404) the Collaborative Education Project for IndustryUniversity Cooperation Supported by the Ministry of Education, and the Introduction (No. 220602817220926) General Research Project on Higher Education Teaching Reform in Heilongjiang Province (No. SJGY20220410).

The author thanks the editors and reviewers for their help and efforts.

Conflict of Interest

The authors declare no conflict of interest.

References

1. YANG F.B., XUE X.Y., CAI C., ZHOU Q.Q., SUN Z. Atomization performance test and influence factors of aviation special centrifugal nozzle. Transactions of the Chinese Society of Agricultural Machinery, **50** (9), 96, **2019**.
2. ZHANG K., ZHAO L., CUI J.Y., MAO P.J., YUAN B.H., LIU Y.Y. Design and Implementation of Evaluation Method for Spraying Coverage Region of Plant Protection UAV. Agronomy, **13** (6), 1631, **2023**.
3. LIU J.P., ZHU X.Y., YUAN S.Q., LIU X.F. Droplet motion model and simulation of a complete fluidic sprinkler. Transactions of the ASABE, **61** (4), 1297, **2018**.
4. TANG Q., ZHANG R.R, CHEN L.P, DENG W., XU M., XU G., LI L.L., HEWITT A. Numerical simulation of the down wash flow field and droplet movement from an unmanned helicopter for crop spraying. Computers and Electronics in Agriculture, **174**, 105468, **2020**.
5. YUAN H.Z., WANG G.B. Effects of droplet size and deposition density on field efficacy of pesticides. Plant protection, **41** (6), 9, **2015**.

6. WANG G.B., HAN Y.X, LI X., ANDALORO J., CHEN P.C., HOFFMANN W.C., HAN X.Q., CHEN S.D., LAN Y.B. Field evaluation of spray drift and environmental impact using an agricultural unmanned aerial vehicle (UAV) sprayer. Science of the Total Environment, **737**, 139793, **2020**.
7. TORRENT X., GREGORIO E., DOUZALS J.P., TINET C., ROSELL-POLO J.R., PLANAS S. Assessment of spray drift potential reduction for hollow-cone nozzles: Part 1. Classification using indirect methods. Science of the Total Environment, **692**, 1322, **2019**.
8. HILZ E., VERMEER A.W.P Spray drift review: The extent to which a formulation can contribute to spray drift reduction. Crop Protection, **44**, 75,**2013**.
9. CHEN S.D., LAN Y.B., ZHOU Z.Y., OUYANG F., WANG G.B., HUANG X.Y., CHENG S.G. Effect of droplet size parameters on droplet deposition and drift of aerial spraying by using plant protection UAV. Agronomy, **10** (2), 195, **2020**.
10. FERGUSON J.C., O'DONNELL C.C., CHAUHAN B.S., ADKINS S.W., KRUGER G.R., WANG R., HEWITT A.J. Determining the uniformity and consistency of droplet size across spray drift reducing nozzles in a wind tunnel. Crop Protection, **76**, 1, **2015**.
11. TIAN L., KUAN P.D., ZUO J.N., SHI Y.Q. Application of integrated system of drip micro-irrigation and fertigation in irrigation of facility agriculture. Modern Agricultural Science and Technology, (01), 153, **2019**.
12. CHEN J., ZHANG D., HE Z., LIU J. Effect of three herbicides on the content of Malondialdehyde and Proline in cotton leaves. Journal of Shihezi University (Nature Science), **30** (1), 33, **2012**.
13. SANTANGELO P.E. Characterization of high-pressure water-mist sprays: Experimental analysis of droplet size and dispersion. Experimental Thermal and Fluid Science, **34** (8), 1353, **2010**.
14. MANDATO S., RONDET E., DELAPLACE G., BARKOUTI A., GALET L., ACCART P., CUQ B. Liquids' atomization with two different nozzles: Modeling of the effects of some processing and formulation conditions by dimensional analysis. Powder technology, **224**, 323, **2012**.
15. ZENG A.J., WANG C.L., SONG J.L., WANG Z.C., HUANG M.Y., HE X.K., HERBST A. Effects of nozzle types, adjuvants and environmental conditions on spray drift potential of unmanned aerial vehicles in a wind tunnel. Chinese Journal of Pesticide Science, **22** (2), 315, **2020**.
16. MCGINTY J.A., BAUMANN P.A., HOFFMANN W.C., FRITZ B.K. Evaluation of the spray droplet size spectra of drift-reducing agricultural spray nozzle designs. American Journal of Experimental Agriculture, **11** (3), 1, **2016**.
17. TORRENT X., GREGORIO E., ROSELL-POLO J.R., ARNO J., PERIS M., VAN DE ZANDE J.C., PLANSA S. Determination of spray drift and buffer zones in 3D crops using the ISO standard and new LiDAR methodologies. Science of the total environment, **714**, 136666, **2020**.
18. LIU Q., WEI K., YANG L., XU W., XUE W. Preparation and application of a thidiazuron· diuron ultra-low-volume spray suitable for plant protection unmanned aerial vehicles. Scientific Reports, **11** (1), 4998, **2021**.
19. BALSARI P., GRELLA M., MARUCCO P., MATTA F., MIRANDA-FUENTES A. Assessing the influence of air speed and liquid flow rate on the droplet size and homogeneity in pneumatic spraying. Pest management science, **75** (2), 366**, 2019**.
20. HAO L., GAO X., CHEN T.Y., WANG H.C. Analysis of flow field of misting nozzle based on ANSYS and parameter optimization. Journal of Agricultural Mechanization Research, **38** (08), 19, **2016**.
21. CARLE F., SEMENOV S., MEDALE M., BRUTIN D. Contribution of convective transport to evaporation of sessile droplets: empirical model. International Journal of Thermal Sciences, **101**, 35, **2016**.
22. VALIULLIN R.T., STRIZHAK A.P. Influence of the shape of soaring particle based on coal-water slurry containing petrochemicals on ignition characteristics. Thermal Science, **21** (3), 1399, **2017**.
23. YAN M.D., JIA W.D., MAO H.P., DONG X., CHEN L. Experimental study on droplet size and velocity distribution of wind curtain spray boom. Transactions of the Chinese Society for Agricultural Machinery, **45** (11), 104, **2014**.
24. ZHANG Z.H., ZENG R.H., LAI Q.H., YUAN S., SHEN S.Y., YANG L. Study on the impact of downwash airflow field of small plant protection UAV on droplet motion characteristics . Transactions of the Chinese Society for Agricultural Machinery, **54** (09), 208, **2023**.
25. ZHANG Y.L., BAI L.C., CHEN P.C., LAN Y.B., YU B.H. Effects of UAV operation parameters on deposition distribution of mist droplets on apple trees. Journal of Agricultural Mechanization Research, **46** (04), 183, **2024**.